FTO promotes ferroptosis through m6A-dependent downregulation of HSPG2 expression in endothelial cell metabolic memory and diabetic nephropathy

Keywords
FTO, diabetic nephropathy, metabolic memory, m6A modification, HSPG2

Abstract
Introduction
Metabolic memory represents a major challenge in diabetic nephropathy (DN), yet the involvement of m6A RNA modification and ferroptosis remains unclear.

Material and methods
Human endothelial cell lines (HUVECs and HRGECs) were used to establish an in vitro model of metabolic memory, alongside a murine model of DN induced by streptozotocin. MeRIP-seq was performed to profile m6A modification in total RNA, and MeRIP-qPCR was conducted to validate m6A enrichment in HSPG2. In HRGECs, gain- and loss-of-function studies for FTO and HSPG2 were carried out prior to induction of metabolic memory. The expression of ferroptosis-related proteins, FTO, and HSPG2 was assessed using real-time PCR, western blotting, and cellular immunofluorescence. Iron dyshomeostasis and oxidative stress were evaluated using commercial kits. Serum samples were analyzed for blood glucose and renal function.

Results
Dysregulation of RNA m6A modification was observed in the endothelial cell metabolic memory model, with a significant downregulation of m6A methylation in HSPG2. Both in vitro and in vivo models exhibited reduced m6A levels and decreased mRNA and protein expression of HSPG2. In contrast, FTO expression was markedly upregulated. Functional analyses demonstrated that FTO suppressed HSPG2 expression in an m6A-dependent manner, thereby promoting ferroptosis. In the mouse model of DN, ferroptosis inhibitor Fer-1 blocked ferroptosis and improved blood glucose and kidney function parameters.

Conclusions
FTO promotes ferroptosis by downregulating HSPG2 expression in an m6A-dependent mechanism and is critically involved in the pathogenesis of endothelial cell metabolic memory and DN. These findings highlight FTO as a potential therapeutic target for DN.

Abstract

Introduction: Metabolic memory represents a major challenge in diabetic nephropathy (DN), yet the involvement of m6A RNA modification and ferroptosis remains unclear.

Materials and methods: Human endothelial cell lines (HUVECs and HRGECs) were used to establish an in vitro model of metabolic memory, alongside a murine model of DN induced by streptozotocin. MeRIP-seq was performed to profile m6A modification in total RNA, and MeRIP-qPCR was conducted to validate m6A enrichment in HSPG2. In HRGECs, gain- and loss-of-function studies for FTO and HSPG2 were carried out prior to induction of metabolic memory. The expression of ferroptosis-related proteins, FTO, and HSPG2 was assessed using real-time PCR, western blotting, and cellular immunofluorescence. Iron dyshomeostasis and oxidative stress were evaluated using commercial kits. Serum samples were analyzed for blood glucose and renal function.

Results: Dysregulation of RNA m6A modification was observed in the endothelial cell metabolic memory model, with a significant downregulation of m6A methylation in HSPG2. Both in vitro and in vivo models exhibited reduced m6A levels and decreased mRNA and protein expression of HSPG2. In contrast, FTO expression was markedly upregulated. Functional analyses demonstrated that FTO suppressed HSPG2 expression in an m6A-dependent manner, thereby promoting ferroptosis. In the mouse model of DN, ferroptosis inhibitor Fer-1 blocked ferroptosis and improved blood glucose and kidney function parameters.

Conclusion: FTO promotes ferroptosis by downregulating HSPG2 expression in an m6A-dependent mechanism and is critically involved in the pathogenesis of endothelial cell metabolic memory and DN. These findings highlight FTO as a potential therapeutic target for DN.

Keywords: diabetic nephropathy, metabolic memory, m6A modification, FTO, HSPG2

Introduction

Diabetic nephropathy (DN) is a prevalent microvascular complication of diabetes and the leading cause of end-stage renal disease (ESRD) worldwide [1, 2]. Early periods of hyperglycemic exposure can induce long-lasting pathological changes that persist despite subsequent restoration of normoglycemia—a phenomenon known as metabolic memory which is closely associated with the progressive development of diabetic complications, including DN [3].

Epigenetic modifications, such as DNA methylation, histone modifications and non-coding RNAs, have been implicated in the underlying mechanisms of metabolic memory [4]. Given their potentially reversible nature, epigenetic alterations have emerged as a key focus in diabetes research, particularly in understanding the persistence of metabolic memory. N6-methyladenosine (m6A), the methylation of adenosine at the N6 position, represents the most abundant internal modification in eukaryotic messenger RNAs [5]. This modification is dynamically regulated by "writers" such as the METTL3–METTL14 complex that catalyze m6A deposition, and “erasers” (e.g., FTO and ALKBH5) that mediate its removal [5]. Accumulating evidence indicates that dysregulation of m6A methylation contributes to the pathogenesis of DN [6-9]. However, whether aberrant m6A methylation plays a role in mediating metabolic memory in diabetes remains unclear.

Ferroptosis is a form of non-apoptotic cell death characterized by redox imbalance, primarily driven by dysregulation of iron homeostasis and excessive lipid peroxidation [10]. Members of the NOX family (NOX1, CYBB/NOX2, and NOX4) contribute to

reactive oxygen species (ROS) generation and thereby promote lipid peroxidation [10]. ACSL4, an enzyme critical in fatty acid metabolism, has been recognized as both a specific biomarker and a functional driver of ferroptosis [10]. The antioxidant enzyme GPX4 serves as a central suppressor of ferroptosis, while ferritin—the iron storage protein composed of ferritin light chain (FTL) and ferritin heavy chain 1 (FTH1)—also plays a protective role against ferroptosis [10]. Growing evidence indicates that ferroptosis may be implicated in the pathogenesis of diabetic complications, including DN [11]. Nevertheless, the underlying connection between ferroptosis and metabolic memory in diabetes remains unclear.

In this study, we aim to investigate the involvement of m6A modification and ferroptosis in metabolic memory using human glomerular endothelial cells (HRGECs) and streptozotocin (STZ)-induced diabetic mouse models.

Materials and methods

Cell culture

Human umbilical vein endothelial cells (HUVECs) (NCACC, Shanghai, China) and human renal glomerular endothelial cells (HRGECs) (BNCC, Beijing, China) were cultured in Dulbecco's modified Eagle medium (DMEM) (Thermo Fisher Scientific, Waltham, MA, USA) supplemented with 10% fetal bovine serum (FBS) (Thermo Fisher Scientific, Waltham, MA, USA) and 1% penicillin/streptomycin. Cells were exposed to normal glucose (NG group, 5 mmol/L) for 6 days, high glucose (HG group, 25 mmol/L) for 6 days, or HG for 3 days followed by normal glucose for 3 days (HN group). The HN group was established as the metabolic memory model according to

previous literature [12].

Methylated RNA immunoprecipitation sequencing (MeRIP-seq) and MeRIP-qPCR

Total RNA was extracted from HUVECs using Trizol reagent and quantified with a Nanodrop ND-1000 spectrophotometer (Thermo Fisher Scientific, Waltham, MA, USA). RNA was then purified using the Dynabead mRNA purification kit (Thermo Fisher Scientific, Waltham, MA, USA) and fragmented with RNA Fragmentation Reagent (Thermo Fisher Scientific, Waltham, MA, USA). m6A-containing RNA fragments were enriched using the EpiMark N6-methyladenosine Enrichment kit (NEB, Ipswich, MA, USA). Briefly, Protein G Dynabeads (Thermo Fisher Scientific, Waltham, MA, USA) were washed with MeRIP buffer and incubated with anti-m6A antibody (NEB) for 2 h at 4°C. The antibody-conjugated beads were subsequently incubated with purified RNA overnight at 4 °C. After washing, m6A-modified RNA was eluted using MeRIP buffer containing 5 mM m6A salt for 30 min at 4 °C. RNA-seq libraries were constructed using the KAPA Stranded mRNA-seq Kit (Illumina, San Diego, CA, USA) and sequenced on an Illumina HiSeq 4000 platform by KangChen Bio-tech (Shanghai, China). Differential m6A peaks (fold change ≥1.5 for up-regulation or ≤ 0.667 for down-regulation, and $P < 0.05$) between the NG and HG or HN groups were subjected to Kyoto Encyclopedia of Genes and Genomes (KEGG) pathway analysis. In parallel, methylated RNA isolated from HRGECs was analyzed by qPCR to assess m6A modification levels in HSPG2.

RNA extraction and qPCR

Total RNA was extracted from cells or tissues using Trizol reagent (Thermo Fisher Scientific, Waltham, MA, USA). The RNA was reverse transcribed into cDNA using a PrimeScript reverse transcription kit (Takara Bio, Shiga, Japan). Quantitative real-time PCR (qRT-PCR) was performed to quantify mRNA expression levels using the SYBR green gene expression assay (Takara Bio, Shiga, Japan) with primers listed in Table S1 and S2. Relative gene expression levels were calculated using the $2^{-\Delta\Delta Ct}$ method, with GAPDH as the internal control.

Western blot analysis

Protein was extracted from cells using RIPA buffer (Thermo Fisher Scientific, Waltham, MA, USA), separated by SDS-PAGE, and transferred to nitrocellulose membranes (Bio-Rad, Hercules, CA, USA). The membranes were incubated overnight at 4°C with primary antibodies against FTO (Thermo Fisher Scientific, Waltham, MA, USA, 27226-1-AP), HSPG2 (Abcam, Cambridge, UK, ab2501), GPX4 (Abcam, Cambridge, UK, ab41787), FTH1 (Zen-Bio, Durham, NC, USA, 381204), NOX1 (Abcam, Cambridge, UK, ab121009), ACSL4 (Invitrogen, Waltham, MA, USA, PA5-27137), and β-actin (Abcam, Cambridge, UK, ab9485). After washing, membranes were incubated with horseradish peroxidase-conjugated secondary antibodies for 1 hour at room temperature. Protein signals were visualized using ECL Western Blotting Substrate (Pierce, Waltham, MA, USA) and quantified with ImageJ software.

Dual-Luciferase Reporter Assay

The full-length coding sequence of human FTO (NCBI RefSeq: NM_001080432.2) was cloned into the pcDNA3.1 vector (Invitrogen, Waltham, MA, USA). A fragment of

the human HSPG2 3' UTR (from NCBI RefSeq: NM_005529.7) was inserted into the pmir-GLO Dual-Luciferase vector (Promega, Madison, WI, USA). HEK293T cells were co-transfected using Lipofectamine 2000 transfection reagent (Invitrogen, Waltham, MA, USA), with the HSPG2-3' UTR reporter plasmid and either the FTO-pcDNA3.1 plasmid or an empty vector control. At 48 hours post-transfection, firefly and Renilla luciferase activities were measured sequentially using the Dual-Luciferase® Reporter Assay System (Promega, Madison, WI, USA). The firefly luciferase signal was normalized to the Renilla luciferase signal for internal control. All transfections and luciferase assays were performed in three independent experiments.

Animal models

All animal experiments in this study were conducted in accordance with the protocols approved by the institutional review board of Shanghai General Hospital, Shanghai Jiao Tong University School of Medicine. Specific pathogen-free (SPF), 10-week-old male C57BL/6 mice were obtained from Shanghai SLAC Laboratory Animal Co. Ltd. Mice were randomly assigned to four groups (n = 6 per group). Mice in the streptozotocin (STZ) and STZ+Fer-1 groups received intraperitoneal injections of STZ (Solarbio, Beijing, China) at a dose of 50 mg/kg body weight per day for five consecutive days, while mice in the control and control+Fer-1 groups received an equal volume of citrate buffer. Mice in the STZ+Fer-1 and the control+Fer-1 groups were administered Fer-1 (Solarbio, Beijing, China) via intraperitoneal injection at a dose of 1 mg/kg body weight per day, continuing until sacrifice. One week after the final STZ injection, blood

glucose levels were measured from the tail vein, and values exceeding 16.7 mmol/L were considered indicative of successful diabetes induction. All mice were fed a high-sugar, high-fat diet with free access to food and water for 12 weeks, and were sacrificed under sodium pentobarbital anesthesia at the end of this period.

Histological analysis

Glomerular damage in kidney tissue was evaluated using hematoxylin and eosin (H&E) staining. Tissue sections were fixed overnight in 10% formalin at room temperature, processed for paraffin embedding, and subsequently sectioned and stained with H&E.

Blood chemistry tests

Blood glucose, urea nitrogen, and serum creatinine levels were measured using an AU5800 automated chemistry analyzer (Beckman Coulter, Brea, CA, USA) one day prior to sacrifice.

Immunofluorescence

HRGECs were fixed with 4% paraformaldehyde, permeabilized with 0.1% Triton (Sigma-Aldrich, St. Louis, MO, USA), and blocked with 10% goat serum. Cells were incubated with primary antibodies against FTO or HSPG2 at 4°C overnight, followed by incubation with fluorescein isothiocyanate (FITC)-conjugated anti-rabbit secondary antibodies for 1 h at room temperature. Nuclei were counterstained with DAPI. Fluorescent images were captured using a fluorescence microscope.

Cell viability assay

Cell viability was assessed using the CCK-8 Cell Proliferation and Cytotoxicity

Assay Kit (Solarbio, Beijing, China) according to the manufacturer's instructions.

Lactate dehydrogenase (LDH) release, total reactive oxygen species (ROS), iron, and malondialdehyde (MDA) assays

LDH release was measured using an LDH Cytotoxicity Assay Kit (Yeasen, Shanghai, China). Total reactive oxygen species (ROS) levels were assessed using a Reactive Oxygen Species Assay Kit (Beyotime, Shanghai, China). Intracellular Fe^{2+} levels were determined using a Ferrous Ion Content Assay Kit (Solarbio, Beijing,China). Malondialdehyde (MDA) levels were quantified using an MDA Content Assay Kit (Solarbio, Beijing, China).

Lentivirus construct transfection

HRGECs were transfected with lentiviral vectors for FTO-overexpression (FTO-OE), or for expressing short hairpin RNAs (shRNAs) targeting FTO (shFTO-1#, shFTO-2#) or HSPG2 (shHSPG2-1#, shHSPG2-2#) using Lipofectamine (Invitrogen, Waltham, MA, USA) according to the manufacturer's instructions. The target sequences for the shRNAs are listed in Table S3.

Statistical analysis

All data were analyzed using GraphPad Prism 8.0. Data are presented as mean ± standard deviation (SD). Statistical differences between two groups were evaluated using Student's t-test. $P < 0.05$ was considered statistically significant.

Results

RNA m6A dysregulation is implicated in metabolic memory

We performed MeRIP-seq to detect m6A methylation profiles in the NG, HG and

HN groups using HUVEC model. Compared with the NG group, 2942 hypermethylated m6A peaks corresponding to 1122 genes and 3930 hypomethylated m6A peaks corresponding to 1470 genes were commonly identified in both the HG and HN groups (Fig. 1A and B). These differentially methylated genes were subjected to KEGG pathway analysis (Fig. 1C and D). Among the m6A hypomethylated genes, the most significantly enriched pathway was "proteoglycans in cancer" (Fig. 1D). Notably, proteoglycans, such as heparan sulfate proteoglycan 2 (HSPG2, also known as perlecan), have been shown to play a critical role in the pathogenesis of diabetic nephropathy [13]. We further examined HSPG2 m6A modification using MeRIP-seq data. Compared with the NG group, m6A methylation in the 3'-untranslated region (3'-UTR) of HSPG2 was significantly reduced in both the HG and HN groups (Fig. 1E).

M6A methylation and expression of HSPG2 are significantly decreased in the in vitro metabolic memory model and in STZ-induced diabetic nephropathy

We next validated HSPG2 m6A methylation using an HRGEC model. MeRIP-qPCR showed that, compared with the NG group, m6A methylation of HSPG2 was significantly reduced in the HN group, although there was a slight recovery relative to the HG group (Fig. 2A). Consistent patterns were observed for HSPG2 mRNA and protein expression levels (Fig. 2B-D). These findings were further confirmed by immunofluorescence staining (Fig. 2E). We then assessed HSPG2 expression in a mouse model of STZ-induced diabetic nephropathy (Fig. S1). Both real-time PCR and western blot analyses demonstrated that HSPG2 expression was substantially downregulated in the STZ-induced mice (Fig. 2F-H).

FTO is highly expressed in metabolic memory in vitro and in STZ-induced diabetic nephropathy

FTO is an m6A demethylase that regulates RNA m6A modification. In vitro experiments using an HRGEC model showed that FTO mRNA expression was the highest in the HG group but remained significantly elevated in the HN group compared to the NG group (Fig. 3A). This expression pattern was confirmed at the protein level by western blot analysis (Fig. 3B and C) and immunofluorescence staining (Fig. 3D), suggesting a potential role of FTO in metabolic memory. We next examined FTO expression in a mouse model of STZ-induced diabetic nephropathy. Both real-time PCR and western blot analyses demonstrated that FTO expression was markedly upregulated in the STZ-induced mice (Fig. 3E-G).

FTO downregulates HSPG2 expression in an m6A-dependent manner in the metabolic memory model of HRGECs

To investigate the regulatory effect of FTO on m6A methylation and expression of HSPG2, we modulated FTO expression in HRGECs, and validated the efficiency of FTO overexpression and knockdown by western blot (Fig. 4A and B). M6A methylation of HSPG2 was reduced upon FTO overexpression and increased upon FTO knockdown (Fig. 4C). Consistently, HSPG2 expression at the mRNA and protein levels exhibited similar trends. FTO overexpression decreased HSPG2 expression, whereas FTO knockdown increased it (Fig. 4D-F). Utilizing dual-luciferase assays, we further demonstrated that FTO targets the 3' UTR region of HSPG2 to suppress its expression (Fig. 4G). We also manipulated HSPG2 expression, with successful modulation

confirmed by western blot (Fig. 4H and I). Notably, the reduction in HSPG2 expression caused by HSPG2 knockdown was partially reversed by co-knockdown of FTO. Furthermore, HSPG2 expression reached its highest level when FTO was knocked down alone (Fig. 4J and K). Collectively, these results indicate that FTO negatively regulates HSPG2 expression in an m6A-dependent manner.

Ferroptosis is involved in metabolic memory in HRGECs

Next, we examined the role of ferroptosis in metabolic memory using an HRGEC model. CCK-8 assay results showed that cell viability was significantly reduced in the HG group compared to the NG group and was not fully restored in the HN group (Fig. 5A). Similar patterns were observed for key ferroptosis-associated parameters, which are characterized by iron dyshomeostasis and oxidative stress. LDH release, ROS levels, intracellular Fe^{2+} concentration, and MDA content were all elevated in the HG group relative to the NG group and remained incompletely normalized in the HN group (Fig. 5B–E). Additionally, the expression of ferroptosis-related proteins GPX4, FTH1, NOX1, and ACSL4 was measured. Compared with the NG group, both real-time PCR and western blot analyses revealed downregulation of GPX4 and FTH1 and upregulation of NOX1 and ACSL4 in both the HG and HN groups, confirming the persistent activation of ferroptotic pathways in metabolic memory (Fig. 5F–H).

HSPG2 knockdown promotes but FTO knockdown inhibits ferroptosis in the metabolic memory model of HRGECs

We subsequently examined the effect of manipulating FTO and/or HSPG2 expression on ferroptosis. Cell viability was significantly decreased upon HSPG2

knockdown. However, co-knockdown of FTO partially restored cell viability (Fig. 6A). To evaluate ferroptosis, we measured LDH release, ROS levels, Fe^{2+} concentration, and MDA content. HSPG2 knockdown increased all four markers, whereas simultaneous FTO knockdown partially attenuated these increases (Fig. 6B-E). Furthermore, HSPG2 knockdown led to downregulation of GPX4 and FTH1 and upregulation of NOX1 and ACSL4 at both mRNA and protein levels. Notably, co-knockdown of FTO partially reversed these changes, mitigating the pro-ferroptotic effects induced by HSPG2 deficiency (Fig. 6F-H).

To further investigate the role of HSPG2 in ferroptosis regulation, we treated cells with the ferroptosis inhibitor Fer-1 following HSPG2 knockdown. Fer-1 significantly attenuated the HSPG2 silencing-induced upregulation of the ferroptosis-associated protein ACSL4 and the downregulation of GPX4 and FTH1 (Fig. 7A-B). Moreover, Fer-1 markedly reduced the elevated levels of LDH, Fe^{2+}, and MDA resulting from HSPG2 knockdown (Fig. 7C-E).

Ferroptosis is involved in diabetic nephropathy induced by STZ

To determine whether ferroptosis is involved in DN, ferrostatin-1 (Fer-1), a specific inhibitor of ferroptosis, was administered to mice with STZ-induced DN. The expression levels of ferroptosis-related markers GPX4, FTH1, NOX1, and ACSL4 were assessed. Fer-1 treatment increased GPX4 and FTH1 levels while decreasing NOX1 and ACSL4 expression in STZ-induced DN mice, although these markers did not fully return to those observed in control mice (Fig. 8A-C). As a result, Fer-1 administration significantly improved blood glucose, blood urea nitrogen, and serum creatinine levels

in STZ-induced mice, although these biochemical parameters remained higher than in the control group (Fig. 8D-F).

Discussion

The present study demonstrated that both RNA m6A dysregulation and ferroptosis are involved in metabolic memory in endothelial cells and DN. Mechanistic studies revealed that FTO promotes ferroptosis by reducing the m6A modification of HSPG2, thereby suppressing its expression in endothelial cells, suggesting that FTO may serve as a promising therapeutic target for the treatment of endothelial cell metabolic memory and DN.

Metabolic memory refers to the sustained dysfunction of target cells or tissues even after glucose levels have been normalized, representing a major challenge in the management of DN [14]. Persistent epigenetic alterations are known to play a critical role in the underlying mechanism of metabolic memory [14]. Accumulating evidence indicates that RNA m6A modification regulates key pathological processes such as inflammation, oxidative stress, fibrosis, and contributes significantly to the onset and progression of DN [15]. In this study, we confirmed that RNA m6A dysregulation is implicated in endothelial cell metabolic memory.

Proteoglycans are synthesized and secreted by glomerular endothelial cells and constitute the major components of the glomerular basement membrane (GBM) [13]. Among the proteoglycans, heparan sulfate proteoglycan 2 (HSPG2, also known as perlecan) carries a negative charge and plays a pivotal role in maintaining the permselectivity of the glomerular barrier [16]. Reduced renal levels of HSPG2 have

been documented in both animal models of DN and diabetic patients, leading to increased glomerular permeability and the development of proteinuria [16]. In this study, KEGG pathway analysis revealed that among m6A hypomethylated genes in the endothelial cell metabolic memory model, the most significantly enriched pathway was "proteoglycans in cancer". Furthermore, m6A methylation levels in the HSPG2 3' UTR were significantly downregulated, which correlated with decreased HSPG2 expression. Notably, it has been reported that m6A modification within the 3' UTR can enhance translational efficiency [17].

FTO is one of the key enzymes regulating m6A demethylation [18]. The level of FTO in the peripheral blood of patients with type 2 diabetes mellitus (T2DM) is elevated, while m6A modification levels in the urine of T2DM patients with DN are significantly reduced [8, 19]. MeRIP sequencing has suggested that FTO may be a key causative factor in endothelial dysfunction of T2DM [20]. High glucose induces FTO expression in human retinal endothelial cells and HUVECs, leading to abnormal endothelial cell function in an m6A-dependent manner [21, 22]. IL-17A promotes endothelial cell senescence by upregulating FTO expression [23]. Statins exert protective effects in endothelial cells by downregulating FTO expression, thereby increasing m6A modification and enhancing the protein expression of KLF2 (Kruppel-like factor 2) and eNOS (endothelial NO synthase) [24].

Elevated FTO levels have been observed in renal tissues of db/db mice, STZ-induced mice, or DN patients [6, 25-27]. However, conflicting findings have also been reported in db/db mice or DN patients [6, 28]. These conflicting reports can be explained by

several context-dependent factors. FTO expression appears to be stage-specific, often transiently elevated in early diabetes but normalizing or even declining in advanced DN. Furthermore, cell-type specificity is crucial, as bulk tissue analyses may obscure distinct expression profiles in different renal cell types. Technical variations in methodology could also contribute to the observed discrepancies. In our study, the consistent upregulation of FTO—observed in both an endothelial cell metabolic memory model and STZ-induced mice—supports its pathogenic role within these specific experimental contexts. We therefore propose that FTO acts as a key m6A regulator driving DN progression. The apparent contradictions in the literature concerning FTO's role ultimately underscore the dynamic complexity of the m6A epigenome in diabetic nephropathy and highlight the importance of defining its precise spatiotemporal regulation.

As an m6A demethylase, FTO post-transcriptionally regulates gene expression by removing m6A modifications, thereby influencing RNA processing, stability, and translation [29]. Notably, one gene whose expression is m6A-sensitive is HSPG2; its m6A-mediated regulation has been associated with hepatitis B virus X protein (HBx)-mediated hepatocarcinogenesis and relapse of acute myeloid leukemia (AML) [30, 31]. In the present study, we revealed that in metabolic memory of endothelial cells, HSPG2 was one of the downstream targets of FTO. The mRNA and protein expression of HSPG2 were downregulated by FTO in an m6A-dependent manner.

Ferroptosis is an iron-dependent form of regulated cell death characterized by iron accumulation and lipid peroxidation [10]. Numerous studies have demonstrated that

high glucose induces ferroptosis in renal intrinsic cells, including renal tubular epithelial cells, podocytes, glomerular endothelial cells, and mesangial cells, contributing to renal injury and DN progression [32]. However, the role of ferroptosis in metabolic memory remains unclear. In this study, we show that ferroptosis is involved in endothelial cell metabolic memory.

Ferroptosis can be precisely regulated at multiple levels, including epigenetic, transcriptional, post-transcriptional, and post-translational levels [10]. Depending on the cellular context, FTO can promote or inhibit ferroptosis by modulating m6A modification of target mRNA [33]. HSPG2 deficiency has been reported to induce endothelial dysfunction through downregulation of endothelial nitric oxide synthase (eNOS) [34]. In cardiomyocytes, inhibition of the Akt/eNOS signaling pathway by miR-199a-5p promotes ferroptosis [35]. In tumor cells, nitric oxide (NO) produced by inducible nitric oxide synthase (iNOS) suppresses ferroptosis by inhibiting lipid peroxidation [36]. Glycosaminoglycans such as HSPG2, which contains an LDLR-like domain, may protect cancer cells from ferroptosis by mediating lipoprotein uptake [37]. Based on these findings, it is reasonable to hypothesize that HSPG2 may inhibit ferroptosis in endothelial cells by regulating NO production and/or lipoprotein uptake. In the present study, we demonstrated that FTO downregulated HSPG2 expression by reducing its m6A modification, thereby promoting ferroptosis in the context of endothelial cell metabolic memory.

Our study has several limitations that merit consideration. First, although our experimental models recapitulate key pathological features, they cannot fully replicate

the complex etiology of human diabetic nephropathy. Second, the clinical translation of our findings faces two major challenges: the broad systemic functions of FTO require kidney-specific delivery systems (e.g., nanoparticle-based targeting) for its small-molecule inhibitors, while the ferroptosis inhibitor Fer-1 is limited by its poor solubility and toxicity profile. Finally, although a functional link between HSPG2 and ferroptosis was established via shRNA knockdown, future studies using orthogonal methods such as CRISPR/Cas9 will be important to definitively rule out off-target effects. Accordingly, future work will focus on developing targeted FTO inhibitors, identifying safer ferroptosis antagonists, and implementing more robust genetic validation strategies.

In conclusion, our findings suggest that FTO contributes to the pathogenesis of endothelial cell metabolic memory and DN by promoting ferroptosis via m6A-dependent downregulation of HSPG2 expression. Thus, FTO represents a potential therapeutic target for DN.

Funding

This study was supported by Natural Science Foundation of Xinjiang Uygur Autonomous Region (Grant No. 2021D01C026).

Conflict of interest

The authors have no conflicts of interest to declare.

Reference

1. Naaman SC, Bakris GL. Diabetic Nephropathy: Update on Pillars of Therapy Slowing Progression. Diabetes Care. 2023; 46(9):1574-1586.

2. Ji C, Zhang C. Causal association between sleep traits and diabetic nephropathy. Archives of Medical Science. 2025. doi: 10.5114/aoms/208530.

3. Chen Z, Natarajan R. Epigenetic modifications in metabolic memory: What are the memories, and can we erase them? Am J Physiol Cell Physiol. 2022; 323(2):C570-C582.

4. Natarajan R. Epigenetic Mechanisms in Diabetic Vascular Complications and Metabolic Memory: The 2020 Edwin Bierman Award Lecture. Diabetes. 2021; 70(2):328-337.

5. Wang S, Lv W, Li T, et al. Dynamic regulation and functions of mRNA m6A modification. Cancer Cell Int. 2022; 22(1):48.

6. Jiang L, Liu X, Hu X, et al. METTL3-mediated m(6)A modification of TIMP2 mRNA promotes podocyte injury in diabetic nephropathy. Mol Ther. 2022; 30(4):1721-1740.

7. Tang W, Zhao Y, Zhang H, Peng Y, Rui Z. METTL3 enhances NSD2 mRNA stability to reduce renal impairment and interstitial fibrosis in mice with diabetic nephropathy. BMC Nephrol. 2022; 23(1):124.

8. Wan SJ, Hua Q, Xing YJ, et al. Decreased Urine N6-methyladenosine level is closely associated with the presence of diabetic nephropathy in type 2 diabetes mellitus. Front Endocrinol (Lausanne). 2022; 13:986419.

9. Li M, Deng L, Xu G. METTL14 promotes glomerular endothelial cell injury and diabetic nephropathy via m6A modification of alpha-klotho. Mol Med. 2021; 27(1):106.

10. Tang D, Chen X, Kang R, Kroemer G. Ferroptosis: molecular mechanisms and health implications. Cell Res. 2021; 31(2):107-125.

11. Yang XD, Yang YY. Ferroptosis as a Novel Therapeutic Target for Diabetes and Its Complications. Front Endocrinol (Lausanne). 2022; 13:853822.

12. Paneni F, Mocharla P, Akhmedov A, et al. Gene silencing of the mitochondrial adaptor p66Shc suppresses vascular hyperglycemic memory in diabetes. Circulation research. 2012; 111(3):278-289.

13. Khramova A, Boi R, Friden V, et al. Proteoglycans contribute to the functional integrity of the glomerular endothelial cell surface layer and are regulated in diabetic kidney disease. Sci Rep. 2021; 11(1):8487.

14. Chen Z, Malek V, Natarajan R. Update: the role of epigenetics in the metabolic memory of diabetic complications. Am J Physiol Renal Physiol. 2024; 327(3):F327-F339.

15. Huang J, Yang F, Liu Y, Wang Y. N6-methyladenosine RNA methylation in diabetic kidney disease. Biomed Pharmacother. 2024; 171:116185.

16. Hiebert LM. Heparan Sulfate Proteoglycans in Diabetes. Semin Thromb Hemost. 2021; 47(3):261-273.

17. Meyer KD. m(6)A-mediated translation regulation. Biochim Biophys Acta Gene Regul Mech. 2019; 1862(3):301-309.

18. Jia G, Fu Y, Zhao X, et al. N6-methyladenosine in nuclear RNA is a major substrate of the obesity-associated FTO. Nat Chem Biol. 2011; 7(12):885-887.

19. Shen F, Huang W, Huang JT, et al. Decreased N(6)-methyladenosine in

peripheral blood RNA from diabetic patients is associated with FTO expression rather than ALKBH5. J Clin Endocrinol Metab. 2015; 100(1):E148-154.

20. Shan L, Tao M, Zhang W, et al. Comprehensive analysis of the m(6)A demethylase FTO in endothelial dysfunction by MeRIP sequencing. Exp Cell Res. 2024; 442(2):114268.

21. Zhou C, She X, Gu C, et al. FTO fuels diabetes-induced vascular endothelial dysfunction associated with inflammation by erasing m6A methylation of TNIP1. J Clin Invest. 2023; 133(19):e160517.

22. Chen X, Wang Y, Wang JN, et al. Lactylation-driven FTO targets CDK2 to aggravate microvascular anomalies in diabetic retinopathy. EMBO Mol Med. 2024; 16(2):294-318.

23. Li N, Luo R, Zhang W, et al. IL-17A promotes endothelial cell senescence by up-regulating the expression of FTO through activating JNK signal pathway. Biogerontology. 2023; 24(1):99-110.

24. Mo W, Chen Z, Zhang X, et al. N6-Methyladenosine Demethylase FTO (Fat Mass and Obesity-Associated Protein) as a Novel Mediator of Statin Effects in Human Endothelial Cells. Arterioscler Thromb Vasc Biol. 2022; 42(5):644-658.

25. Lu Z, Liu H, Song N, et al. METTL14 aggravates podocyte injury and glomerulopathy progression through N(6)-methyladenosine-dependent downregulating of Sirt1. Cell Death Dis. 2021; 12(10):881.

26. Fu K, Jing C, Shi J, et al. WTAP and METTL14 regulate the m6A modification of DKK3 in renal tubular epithelial cells of diabetic nephropathy. Biochem

Biophys Res Commun. 2024; 738:150524.

27. Wu H, Yu Z, Yang Y, et al. The impact of METTL3 on MDM2 promotes podocytes injury during diabetic kidney disease. J Cell Mol Med. 2025; 29(10):e70627.

28. Sun Q, Geng H, Zhao M, et al. FTO-mediated m(6) A modification of SOCS1 mRNA promotes the progression of diabetic kidney disease. Clin Transl Med. 2022; 12(6):e942.

29. Li Y, Su R, Deng X, Chen Y, Chen J. FTO in cancer: functions, molecular mechanisms, and therapeutic implications. Trends Cancer. 2022; 8(7):598-614.

30. Sivasudhan E, Zhou J, Ma J, et al. Hepatitis B Virus X Protein Contributes to Hepatocellular Carcinoma via Upregulation of KIAA1429 Methyltransferase and mRNA m6A Hypermethylation of HSPG2/Perlecan. Mol Carcinog. 2025; 64(1):108-125.

31. Zhang J, Liu T, Wang Y, et al. Dynamic alterations of the transcriptome-wide m(6)A methylome in cytogenetically normal acute myeloid leukaemia during initial diagnosis and relapse. Genomics. 2023; 115(6):110725.

32. Wu Q, Huang F. Targeting ferroptosis as a prospective therapeutic approach for diabetic nephropathy. Ann Med. 2024; 56(1):2346543.

33. Tao X, Kang N, Zheng Z, Zhu Z, Ma J, He W. The regulatory mechanisms of N6-methyladenosine modification in ferroptosis and its implications in disease pathogenesis. Life Sci. 2024; 355:123011.

34. Nonaka R, Iesaki T, de Vega S, et al. Perlecan deficiency causes endothelial

dysfunction by reducing the expression of endothelial nitric oxide synthase. Physiol Rep. 2015; 3(1):e12272.

35. Zhang GY, Gao Y, Guo XY, Wang GH, Guo CX. MiR-199a-5p promotes ferroptosis-induced cardiomyocyte death responding to oxygen-glucose deprivation/reperfusion injury via inhibiting Akt/eNOS signaling pathway. Kaohsiung J Med Sci. 2022; 38(11):1093-1102.

36. He Q, Qu M, Xu C, et al. The emerging roles of nitric oxide in ferroptosis and pyroptosis of tumor cells. Life Sci. 2022; 290:120257.

37. Calhoon D, Sang L, Bezwada D, et al. Glycosaminoglycan-driven lipoprotein uptake protects tumours from ferroptosis. Nature. 2025; 644(8077):799-808.

Figure Legends

Figure 1. M6A dysregulation is involved in metabolic memory in human umbilical vein endothelial cells (HUVECs). (A and B) Venn diagrams showing the number of differential m6A peaks shared between the HG and HN groups compared to the NG group (fold change ≥ 1.5 for up-regulation or ≤ 0.667 for down-regulation, $p < 0.05$). (C and D) KEGG pathway analysis results for genes associated with differentially methylated m6A peaks. (E) HSPG2 m6A methylation levels in the HG and HN groups relative to the NG group. Data are presented as mean ± SD (n = 3 independent experiments). $^{**}p < 0.01$ vs. NG group.

Figure 2. M6A modification and expression of HSPG2 are markedly reduced in metabolic memory in human renal glomerular endothelial cells (HRGECs) and streptozotocin (STZ)-induced diabetic nephropathy. (A) HSPG2 m6A methylation levels measured by MeRIP-qPCR in NG, HG, and HN groups. (B-E) HSPG2 expression analyzed by real-time PCR (B), western blot (C and D), and immunofluorescence (E; original magnification, ×200) in NG, HG, and HN groups. (F-H) HSPG2 expression in kidney tissues from control and STZ-induced mice determined by real-time PCR (F) and western blot (G and H). Data are presented as mean ± SD (n = 3 independent experiments for in vitro studies; n = 3 mice per group for in vivo studies). $^{*}p < 0.05$, $^{**}p < 0.01$ vs. NG group or control group.

Figure 3. FTO is highly expressed in metabolic memory in human renal glomerular endothelial cells (HRGECs) and in streptozotocin (STZ)-induced diabetic nephropathy. (A-D) FTO expression assessed by real-time PCR (A), western blot (B and C), and immunofluorescence (D; original magnification, ×200) in NG, HG,

and HN groups. (E-G) FTO expression in kidney tissues from control and STZ-induced mice evaluated by real-time PCR (E) and western blot (F and G). Data are presented as mean ± SD (n = 3 independent experiments for in vitro studies; n = 3 mice per group for in vivo studies). *$p < 0.05$, **$p < 0.01$ vs. NG group or control group.

Figure 4. FTO downregulates m6A methylation and expression of HSPG2 in metabolic memory in human renal glomerular endothelial cells (HRGECs). (A and B) Western blot confirming the efficiency of FTO overexpression (FTO-OE) and knockdown (sh-FTO). (C) HSPG2 m6A methylation levels quantified by MeRIP-qPCR. (D-F) HSPG2 expression of HSPG2 measured by real-time PCR (D) and western blot (E and F). (G) The dual-luciferase assay confirmed that FTO represses the 3' UTR activity of HSPG2. (H and I) Western blot validation of HSPG2 knockdown efficiency (sh-HSPG2). (J and K) Western blot analysis of HSPG2 expression in the rescue experiments. Data are presented as mean ± SD (n = 3 independent experiments). *$p < 0.05$, **$p < 0.01$.

Figure 5. Ferroptosis plays a role in metabolic memory in human renal glomerular endothelial cells (HRGECs). (A) Cell viability assessed by CCK-8 assay in NG, HG, and HN groups. (B-E) Ferroptosis markers evaluated by LDH release (B), ROS levels (C), Fe^{2+} (D), and MDA content (E) were measured to assess ferroptosis. (F-H) Expression of ferroptosis-related proteins (GPX4, FTH1, NOX1, ACSL4) analyzed by real-time PCR (F) and western blot (G and H). Data are presented as mean ± SD (n = 3 independent experiments). **$p < 0.01$ vs. NG group.

Figure 6. FTO knockdown partially counteracts the pro-ferroptotic effect of

HSPG2 knockdown in metabolic memory in human renal glomerular endothelial cells (HRGECs). (A) Cell viability measured by CCK-8 assay. (B-E) Ferroptosis markers including LDH release (B), ROS levels (C), Fe^{2+} (D), and MDA content (E). (F-H) Expression of ferroptosis-related proteins (GPX4, FTH1, NOX1, and ACSL4) determined by real-time PCR (F) and western blot (G and H). Data are presented as mean ± SD (n = 3 independent experiments). *$p < 0.05$, **$p < 0.01$.

Figure 7. HSPG2 modulates ferroptosis in metabolic memory in human renal glomerular endothelial cells (HRGECs). (A and B) Western blot analysis of the ferroptosis-related proteins (GPX4, FTH1, and ACSL4). (C-E) Assessment of ferroptosis by measuring LDH release (C), Fe^{2+} levels (D), and MDA content (E). Data are presented as mean ± SD (n = 3 independent experiments). **$p < 0.01$.

Figure 8. Ferroptosis is implicated in streptozotocin-induced diabetic nephropathy. (A-C) Expression of ferroptosis-related markers (GPX4, FTH1, NOX1, and ACSL4) measured by real-time PCR (A) and western blot (B and C). (D-F) Blood glucose (D), blood urea nitrogen (E), and serum creatinine (F) in control and STZ-induced mice.. Data are presented as mean ± SD (n = 3 mice per group). *$p < 0.05$, **$p < 0.01$ vs. control mice; $^{\$}p < 0.05$, $^{\#}p < 0.01$ vs. STZ-induced mice.

FTO promotes ferroptosis via m6A-dependent HSPG2 downregulation in Diabetic Nephropathy

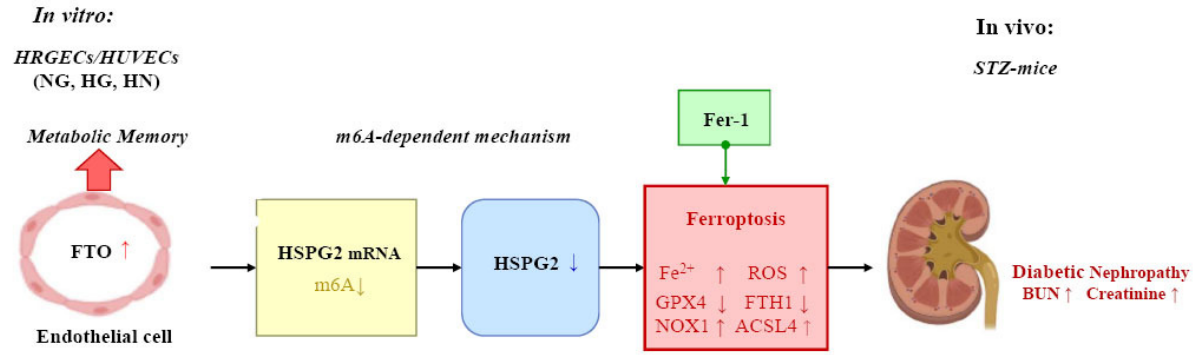

Validated in:
HRGEC metabolic memory model
STZ-induced diabetic mice

Key findings:
FTO ↑ in metabolic memory
HSPG2 ↓ via m6A mechanism
Promotes ferroptosis

Therapeutic implication:
FTO as potential target
Fer-1 improves outcomes

HRGECs: human renal glomerular endothelial cells; HUVECs: human umbilical vein endothelial cells; STZ: streptozotocin; NG: normal glucose (NG group, 5 mmol/L); HG:high glucose (HG group, 25 mmol/L); HN: *the metabolic memory model.*

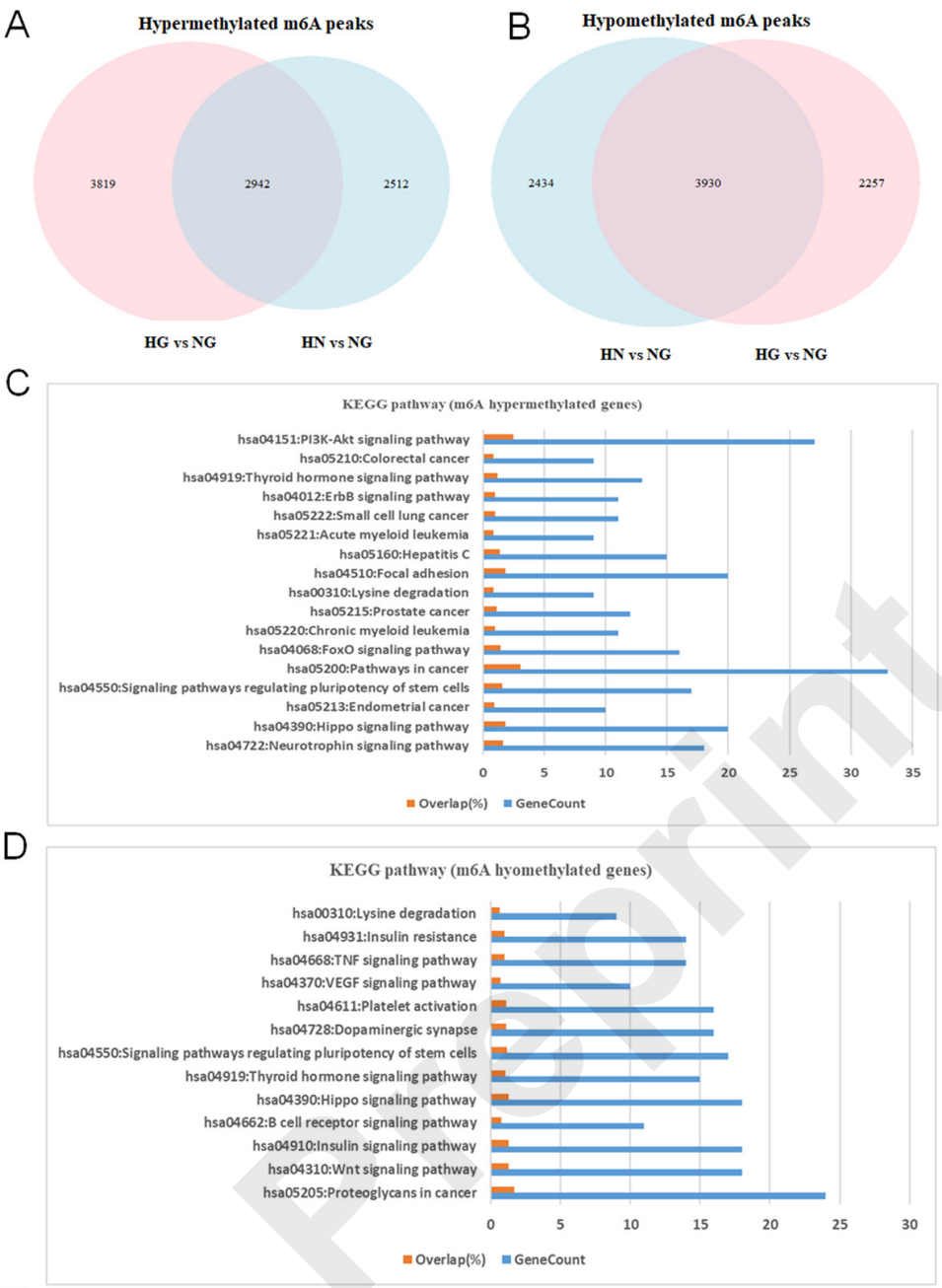

E

HG vs NG

Chromosome	Peak_start	Peak_end	Gene_name	fold_change	Peak_region
chr1	22148737	22148978	HSPG2	0.652477	utr3

HN vs NG

Chromosome	Peak_start	Peak_end	Gene_name	fold_change	Peak_region
chr1	22148737	22148948	HSPG2	0.617709	utr3

Figure 1. M6A dysregulation is involved in metabolic memory in human umbilical vein endothelial cells (HUVECs).

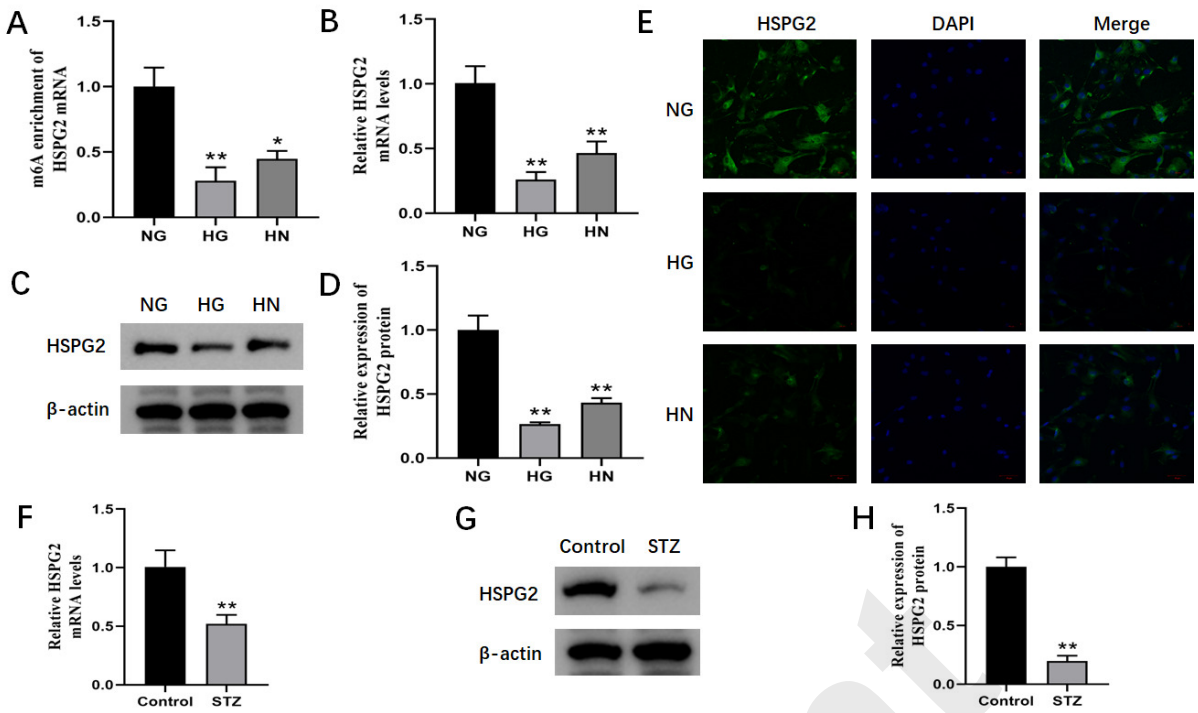

Figure 2. M6A modification and expression of HSPG2 are markedly reduced in metabolic memory in human renal glomerular endothelial cells (HRGECs) and streptozotocin (STZ)-induced diabetic nephropathy.

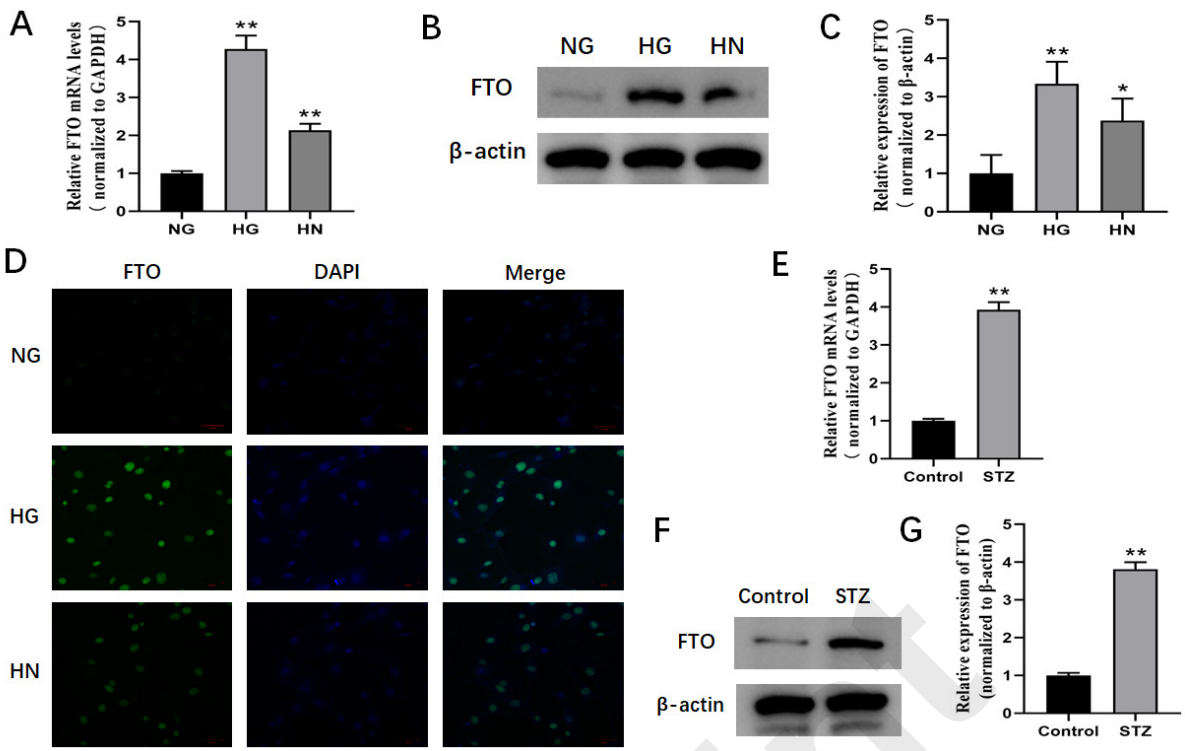

Figure 3. FTO is highly expressed in metabolic memory in human renal glomerular endothelial cells (HRGECs) and in streptozotocin (STZ)-induced diabetic nephropathy.

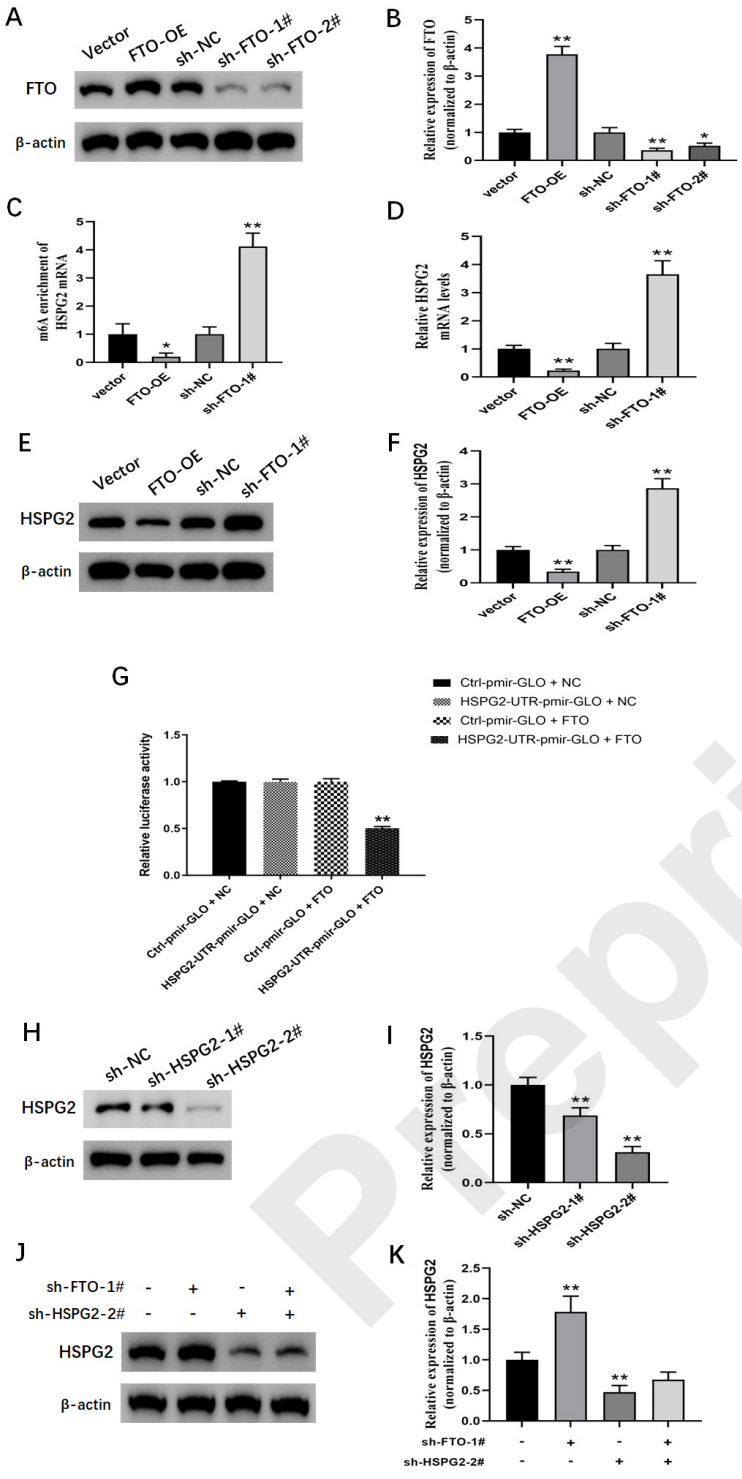

Figure 4. FTO downregulates m6A methylation and expression of HSPG2 in metabolic memory in human renal glomerular endothelial cells (HRGECs).

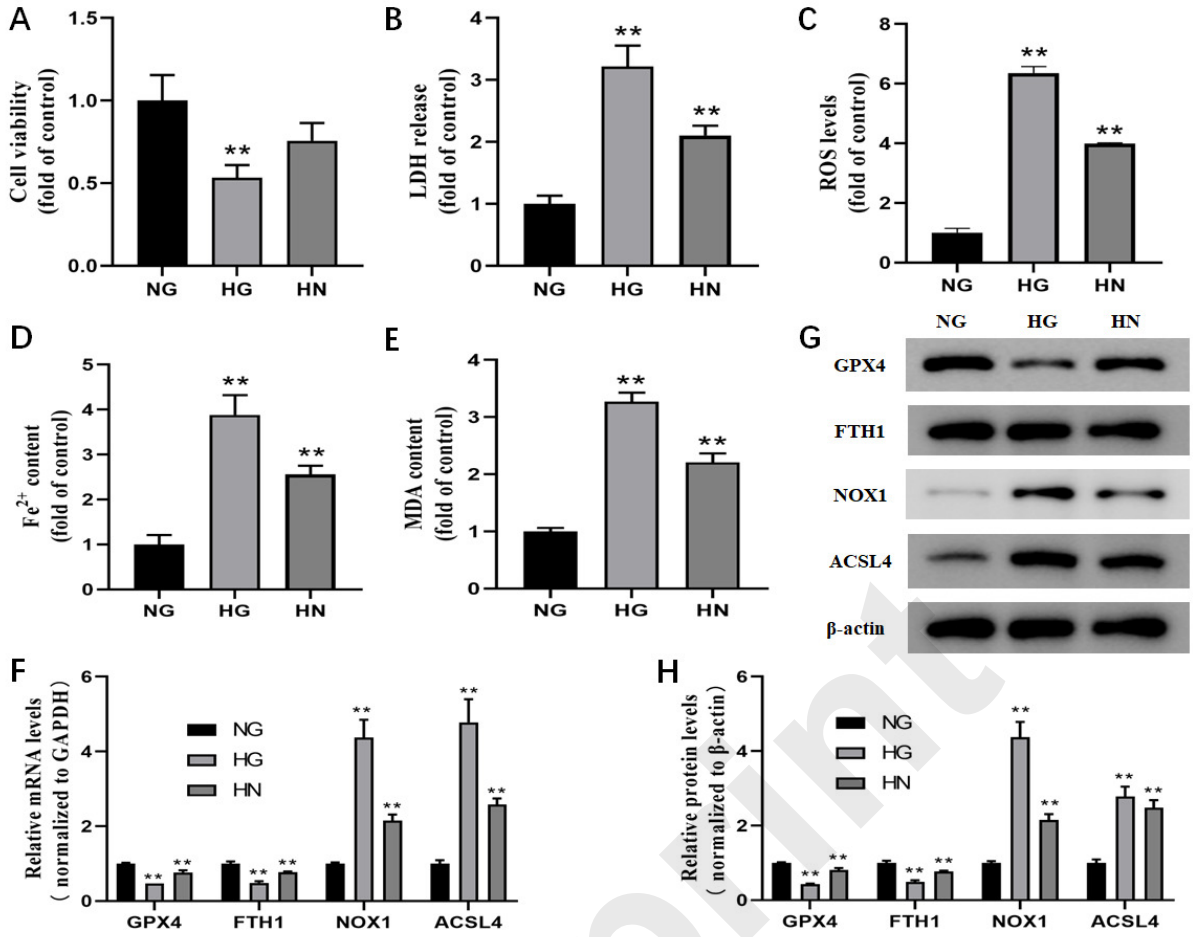

Figure 5. Ferroptosis plays a role in metabolic memory in human renal glomerular endothelial cells (HRGECs).

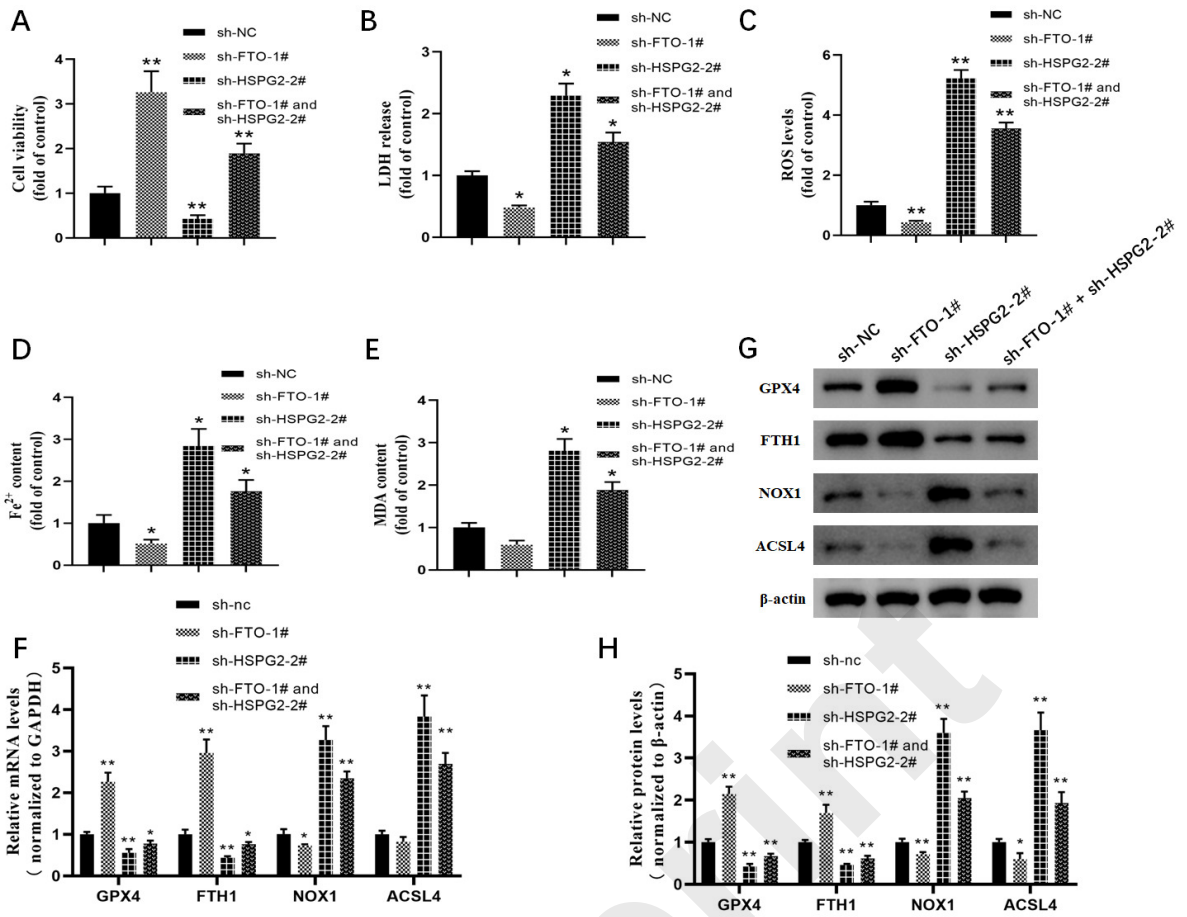

Figure 6. FTO knockdown partially counteracts the pro-ferroptotic effect of HSPG2 knockdown in metabolic memory in human renal glomerular endothelial cells (HRGECs).

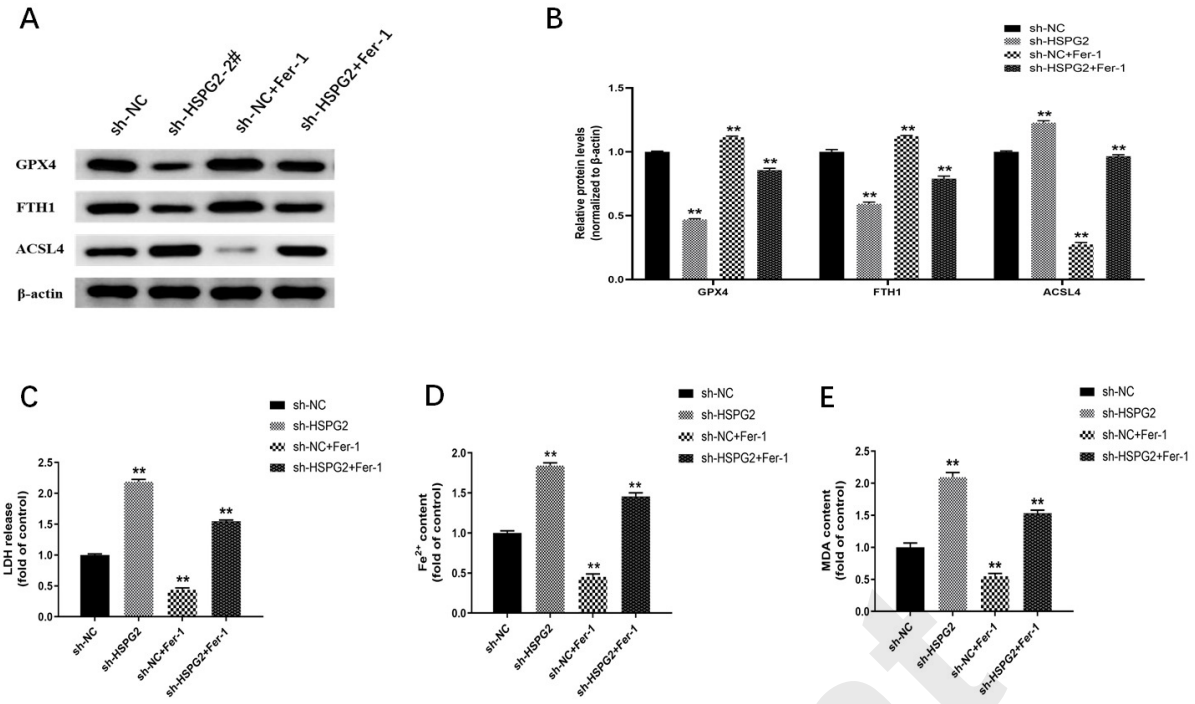

Figure 7. HSPG2 modulates ferroptosis in metabolic memory in human renal glomerular endothelial cells (HRGECs).

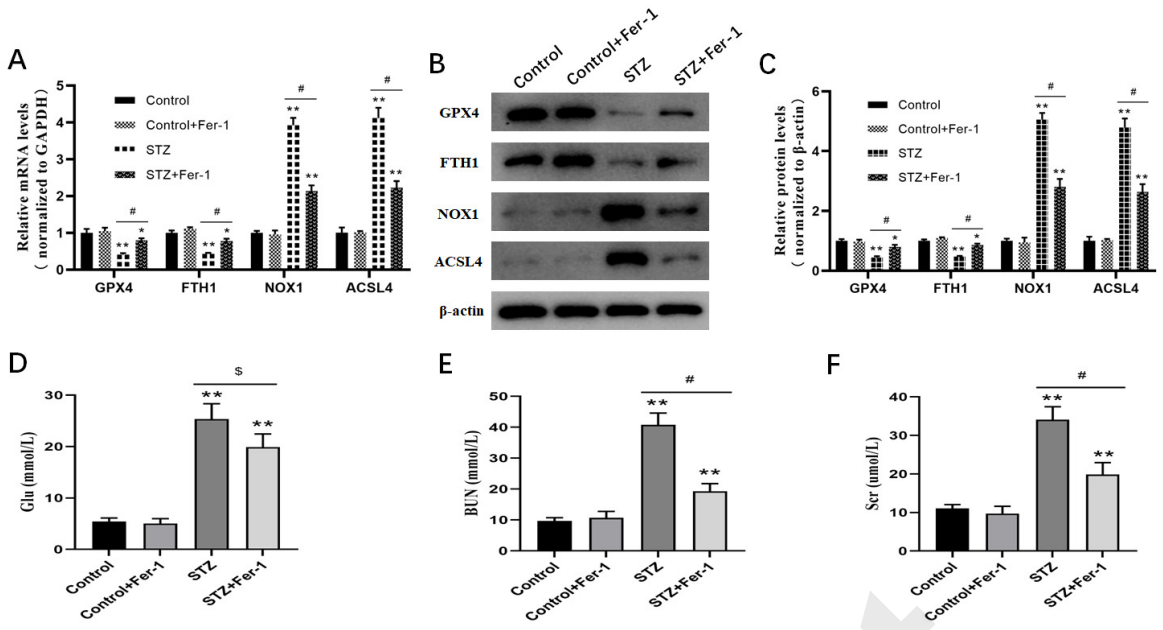

Figure 8. Ferroptosis is implicated in streptozotocin-induced diabetic nephropathy.